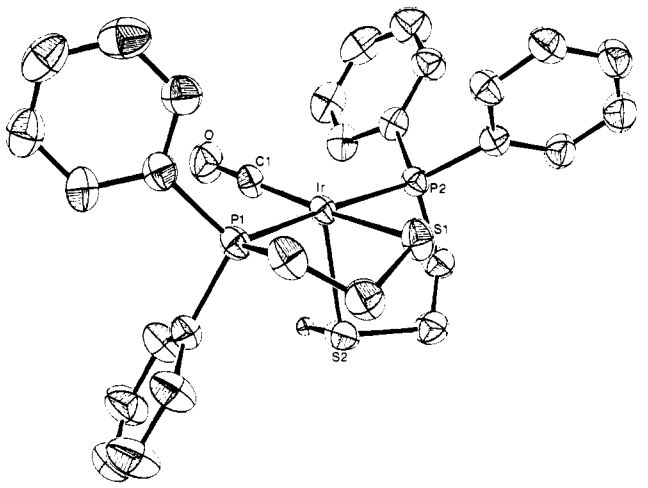

Figure 2. ORTEP view of the cation $[IrH(PS)(PSH)(CO)]^+$. 50% probability thermal ellipsoids are drawn.

$(PPh_3)(PS)(CO)Cl$ (**3**). This Ir(III) species arises from a reaction involving oxidative addition of thiol to Ir(I) and substitution of the more basic phosphine in PSH for PPh_3. In similar reactions involving phosphine–acid or phosphine–aldehyde chelates, Rauchfuss[26] showed that phosphine replacement following chelate-assisted oxidative addition was the reaction sequence leading to the P–O chelate analogues of **3**.

Ir(III) species containing hydride and thiolate ligands are known to be unstable,[25] readily undergoing reductive elimination of HCl, generating an Ir(I) product. We conclude that reductive elimination of HCl from **3** generates the observed equilibrium concentration of the Ir(I) species (**2**) in our reaction mixture.

Reaction of **1** with more than 1 equiv of PSH was performed in CH_2Cl_2. On slow addition of hexane, colorless crystalline blocks of **4** formed. The ^{31}P NMR spectrum of a solution of this compound contained two doublets with chemical shift values distinct from those corresponding to **1**, **2**, or **3**. This is consistent with a new Ir species with two inequivalent P atoms. The $^2J_{P-P}$ value is consistent with a trans arrangement of the P atoms. ^1H NMR data showed a doublet of doublets at −11.7 ppm, consistent with an Ir–H species. IR data contained an absorbance at 2142 cm^{-1}, which was assigned to ν_{Ir-H}. An absorbance assigned to ν_{CO} was observed at 2042 cm^{-1}. The integration of the ^1H NMR signals revealed the presence of an additional H signal masked by the methylene envelope. In addition to these spectroscopic data the combustion analysis was consistent with our formulation of **4** as $[IrH(PS)(PSH)(CO)]^+Cl^-$.

Confirmation of the formulation of **4** was obtained from an X-ray crystallographic investigation. The study clearly showed that the crystal is built from unit cells each containing discrete cations and anions, as is evident from the Ir···Cl distance of 4.562 Å. The closest nonbonded contact between cation and anion is Cl···H(S2), 2.056 Å. This interaction is consistent with hydrogen bonding between the coordinated thiol and the anion. Selected interatomic dimensions are given in Table IV. An ORTEP drawing of the cation is shown in Figure 2. The geometry of Ir as determined from the X-ray experiment is best described as a distorted square-based pyramid, with a coordination sphere consisting of the ligands CO, PS, and PSH. The hydride hydrogen atom was not located; however, the geometry at Ir is consistent with spectroscopic evidence for an Ir–H species. The hydride ligand completes the octahedral coordination of Ir(III) in **4**. The coordination of the thiol group of PSH suggested from the formulation of **4** as an Ir(III) species is confirmed by the location of the thiol hydrogen atom H(S2). The S2–H(S2) distance, 1.35 Å, is consistent with that expected for a S–H bond.[27] The P atoms of the PS and PSH ligands are in a trans orientation, while the thiolate sulfur of PS is trans to CO and the thiol sulfur of PSH is trans to hydride. The bite angles of the two P–S chelates are similar, averaging 85.1°, typically of five-membered chelate rings.[28] Ir–P, Ir–S, and Ir–C bond distances are typical of those observed in other systems.[29] The difference in the Ir–S bond distances (2.411 (1) vs. 2.462 (1) Å) reflects the difference of thiolate vs. thiol coordination as well as the trans influence of CO vs. H. Consequently, direct comparison of Ir–SR and Ir–HSR bond distances cannot be made.

The mechanism of formation of species **4** is a subject for speculation. An obvious route to this compound would involve a phosphine exchange reaction of PSH with **3**, displacing PPh_3. The chelate effect of PSH together with the strong trans effect of hydride could then result in displacement of chloride, yielding **4**.

The species **4** represents the first organometallic species in which thiol coordination has been observed. Other species in which M–HSR coordination have been fully documented are limited to porphyrin complexes of Ru,[30] Fe,[31] and Zn.[32] Clearly, the chelating nature of the mixed phosphorus–sulfur ligand (PSH) assists in stabilizing the novel thiol coordination described herein. Other aspects of the chemistry of mixed-donor ligands are currently under examination and will be reported in due course.[33]

Acknowledgment. We acknowledge the financial support of the President's Research Board of the University of Windsor and the NSERC of Canada.

Registry No. **1**, 15318-31-7; **2**, 90481-52-0; **3**, 90481-53-1; **4**, 90481-54-2.

Supplementary Material Available: Tables S-I–S-IV, listing temperature factors, hydrogen atom parameters, angles and distances associated with phenyl rings, and observed and calculated structure factors (29 pages). Ordering information is given on any current masthead page.

(26) Landvatter, E. F.; Rauchfuss, T. B. *Organometallics* **1982**, *1*, 506.
(27) Kennard, O. "Handbook of Chemistry and Physics", 54th ed.; CRC Press: Cleveland, OH, 1974; p F-198.
(28) Payne, N. C.; Ball, R. G. *Inorg. Chem.* **1977**, *16*, 1187.
(29) Kubiak, C. P.; Woodcock, C.; Eisenberg, R. *Inorg. Chem.* **1980**, *19*, 2733.
(30) Kuehn, C. G.; Taube, H. *J. Am. Chem. Soc.* **1976**, *98*, 689.
(31) Collman, J. P.; Sorrell, T. N.; Hodgson, K. O.; Kulshrestha, A. K.; Strause, C. E. *J. Am. Chem. Soc.* **1977**, *99*, 5180.
(32) Nappa, M.; Valentine, J. S. *J. Am. Chem. Soc.* **1978**, *100*, 5675.
(33) White, G. S.; Stephan, D. W., unpublished results.
(34) Vaska, L.; DiLuzio, J. W. *J. Am. Chem. Soc.* **1961**, *83*, 2784.

Contribution from the Radiation Laboratory, University of Notre Dame, Notre Dame, Indiana 46556

Mechanistic Organometallic Photochemistry: Observation of Metastable Ruthenocenium in Photolysis of Ruthenocene

J. Granifo and G. Ferraudi*

Received August 5, 1983

The photochemistry of ruthenocene, $Ru(cp)_2$,[1] in halogenated hydrocarbons has been investigated by several groups, which agreed on the redox nature of the photochemical processes.[2,3] Unfortunately, doubts on the assignments of the

(1) Throughout this work the symbol Cp stands for η-C_5H_5.

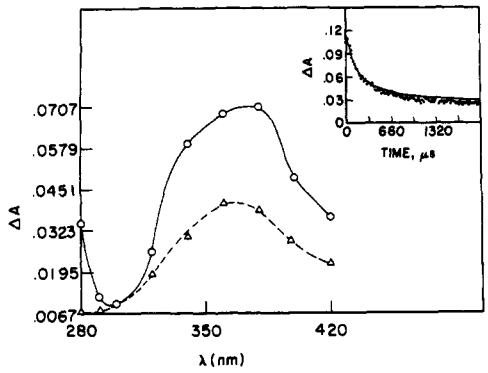

Figure 2. Differential spectra of $Ru(cp)_2Cl$ (solid line) and $Ru(cp)_2Cl^+$ (dashed line) obtained in flash photolysis of $Ru(cp)_2$, $\lambda_{excit} \geq 300$ nm, in deaerated CCl_4. The spectra of $Ru(cp)_2Cl$ and $Ru(cp)_2Cl^+$ were determined with 100- and 700-μs delays, respectively, after a flash irradiation of 30 μs. The inset shows a typical average of five traces (dotted curve) with a second-order curve fitting (solid line).

reaction product as ruthenocenium, $Ru(cp)_2^+$, have been cast by electrochemical[4,5] and crystallographic[6] studies which show that the photochemical product is likely a two-electron oxidation derivative of ruthenocene, e.g., $Ru(cp)_2Cl^+$.[7] Insofar as these studies suggested that ruthenocenium could be very unstable under the experimental conditions of the photochemical experiments, it was clear that the information on the mechanism of the photochemical reaction had to be reevaluated. We found that flash photolysis could be conveniently applied to this mechanistic problem in order to observe fast reactions of the intermediates like the disproportionation of ruthenocenium into the stable two-electron oxidized product.

Results and Discussion

The 280-nm continuous photolysis of $Ru(cp)_2$ in deaerated CCl_4, where 10% of the ruthenium complex forms an adduct with carbon tetrachloride,[3b,8] induces spectral changes that can be related to the formation of the two-electron oxidized product, $Ru(cp)_2Cl^+$. Indeed, we found that these spectral transformations (Figure 1)[10] in good agreement with those expected for mixtures of ruthenocene and $Ru(cp)_2Cl^+$.[9] For this comparison of the spectral properties, we obtained the spectra of the two-electorn oxidized species, $Ru(cp)_2X^+$ with X = Cl or Br, in electrochemical oxidations of ruthenocene in deaerated acetonitrile (Figure 1).[10] It must be pointed out that the spectrum of $Ru(cp)_2Br^+$ with Br_3^- as a counterion was in very good agreement with one previously reported by Gray and co-workers.[5]

Our observations based on the photoinduced spectral transformations demonstrated that, contrary to earlier reports,[2,3b] the first stable product of the photochemical reaction (in deaerated CCl_4 with $\lambda_{excit} = 280$ nm and $I_0 \approx 4 \times 10^{-5}$ einstein/(dm^3 min)) is $Ru(cp)_2Cl^+$ and not the ruthenocenium ion. Therefore, the formation of the two-electron oxidized complex was time resolved by conventional and laser flash photolysis in order to gain some insight of the reaction mechanism. Spectral transformations, followed in a nanosecond–microsecond time scale with our laser flash photolysis unit, revealed the formation of a precursor of $Ru(cp)_2Cl^+$ at times shorter than the time resolution of our apparatus, e.g. ~10 ns. This precursor has a differential absorption spectrum with a maximum at 360 nm (Figure 2) and suffers no transformations at reaction times shorter than 1 μs. The transformation of the precursor into the stable $Ru(cp)_2Cl^+$ was observed in a milisecond time scale (Figure 2). Indeed, the difference spectrum obtained after the complete decay of the transient, e.g. $t > 1$ s, was the one expected for the formation of $Ru(cp)_2Cl^+$. The rate of the transformation of the precursor, determined as a function of the precursor concentration and investigated by appropriate curve fitting, exhibited second-order kinetics which was not affected by various radical scavengers (Table I). This suggests that the precursor assigned as ruthenocenium, $Ru(cp)_2Cl$, disproportionates into ruthenocene and $Ru(cp)_2Cl^+$. Henceforth the photochemical transformations, induced by irradiation of the adduct $Ru(cp)_2 \cdot CCl_4$, can be more correctly described by eq 1–4 than

$$Ru(cp)_2 \cdot CCl_4 \xrightleftharpoons{h\nu} CT \rightarrow Ru(cp)_2Cl + \cdot CCl_3 \quad (1)$$

$$t_{1/2} \leq 10 \text{ ns}$$

$$2Ru(cp)_2Cl \rightarrow Ru(cp)_2 + Cl^- + Ru(cp)_2Cl^+ \quad (2)$$

$$k = 3.2 \times 10^9 \text{ M}^{-1} \text{ s}^{-1}$$

by previously proposed mechanisms.[11] Under the experimental conditions of flash photolysis, that is to say high concentrations of the products of reaction 1 and low concentrations of ruthenocene, the reaction of the trichloromethyl radical with ruthenocene (eq 3) was almost beyond detection, and we can

$$\cdot CCl_3 + Ru(cp)_2 \xrightarrow[H^+]{} Ru(cp)_2^+ + HCCl_3 \quad (3)$$

$$\cdot CCl_3 + Ru(cp)_2Cl \rightarrow Ru(cp)_2 \cdot CCl_4 \quad (4)$$

$$\cdot CCl_3 + \cdot CCl_3 \rightarrow C_2Cl_6 \quad (5)$$

only make it accountable for small deviations from a second-order kinetics in the decay of ruthenocenium (Figure 2).

Table I. Rates of Disproportionation of $Ru(cp)_2Cl$ into $Ru(cp)_2Cl^+$

conditions[a]	C_0,[b] M	$10^{-3}kC_0$,[c] s^{-1}
	7.9×10^{-7}	3.7 ± 0.3
	1.6×10^{-6}	7.0 ± 0.3
7.7×10^{-2} M HCl	1.4×10^{-6}	6.6 ± 0.2
5.0×10^{-2} M C_2H_4	1.4×10^{-6}	5.6 ± 0.2
1.0×10^{-2} M O_2	1.5×10^{-6}	4.7 ± 0.1

[a] All these reactions were run in CCl_4. Solutions were deaerated with streams of Ar unless specially stated. [b] The initial concentration of $Ru(cp)_2Cl$ was estimated from a mass balance, $C_0 = [Ru(cp)_2Cl]_{t\rightarrow 0} = 2[Ru(cp)_2Cl^+]_{t\rightarrow\infty}$, and an extinction coefficient $\epsilon = 1.28 \times 10^3$ M^{-1} cm^{-1} for $Ru(cp)_2Cl^+$ at 360 nm. [c] Product of the initial concentration of ruthenocenium, $[Ru(cp)_2Cl]_{t\rightarrow 0} = C_0$, and the second-order rate constant, k. Each kC_0 value was obtained as a least-squares fit of 100 data points from an average of more than 5 traces.

(2) Traverso, O.; Sostero, S.; Mazzocchin, G. A. *Inorg. Chim. Acta* **1974**, *11*, 237.
(3) (a) Borrel, P.; Henderson, E. *Inorg. Chim. Acta* **1975**, *12*, 215. (b) Borrell, P.; Henderson, E. *J. Chem. Soc., Dalton Trans.* **1975**, 432.
(4) Denisovich, L. I.; Zakurin, N. V.; Bezrukova, A. A.; Gubin, S. P. *J. Organomet. Chem.* **1974**, *81*, 207.
(5) Hendrickson, D. N.; Sohn, Y. S.; Morrison, W. H.; Gray, H. B. *Inorg. Chem.* **1972**, *11*, 808.
(6) Sohn, Y. S.; Schlueter, A. W.; Hendrickson, D. N.; Gray, H. B. *Inorg. Chem.* **1974**, *13*, 301.
(7) Questions about the assignment of the photochemical product were initially raised in lines 2–4 of: Watts, W. E. *Organomet. Chem.* **1975**, *4*, 369.
(8) The ruthenocene–carbon tetrachloride adduct has been designated as $Ru(cp)_2 \cdot CCl_4$ in the text.
(9) Conversions to products were maintained below 1% of the ruthenocene concentration in order to avoid photolysis of the product. With this precaution, the 380-nm absorbance increased due to the formation of $Ru(cp)_2Cl^+$ and the increments were proportional to the irradiation time.
(10) Supplementary material.
(11) CT in eq 1 represents the reactive charge-transfer state.[1-3] It must be noticed that it is possible for ruthenocene and CCl_4 to be associated through the aromatic cyclopentadienyl ring. This type of adduct must be closely related to Mulliken's molecular complexes,[12] and the ruthenocene–CCl_4 charge-transfer transition at 280 nm can be described as $Cl_{p\pi} \rightarrow cp_{\pi^*}$ in a zero-order approximation.
(12) Mulliken, R. S. *J. Phys. Chem.* **1952**, *56*, 801 and references therein.

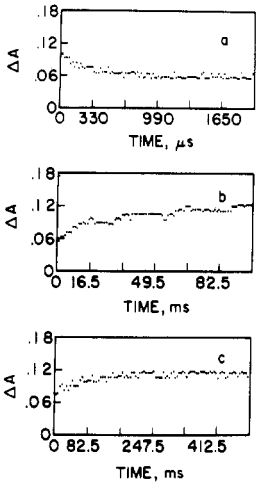

Figure 3. Three instants in the spectral transformations induced by the flash irradiation of $Ru(cp)_2$ in oxygenated ($[O_2] \approx 1.0 \times 10^{-2}$ M) CCl_4. These traces correspond to the disproportionation of $Ru(cp)_2Cl$ into $Ru(cp)_2Cl^+$ (a) and the formation of products in reactions of oxygenated radicals with ruthenocene (b, c).

Moreover, reactions between the trichloromethyl radical and ruthenocenium such as eq 4 can be ruled out because scavengers of the radical have no effect on the reaction kinetics (Table I).

The photochemical generation of trichloromethyl radicals, which were optically transparent at those wavelengths available for the investigation of the reaction intermediates, was verified in aerated solutions. Flash photolysis of $Ru(cp)_2 \cdot CCl_4$ produces (in addition to $Ru(cp)_2Cl$) a new product(s) (Figure 3) that is very likely generated in reactions between ruthenocene and oxygenated radicals such as trichloromethylsuperoxy or trichloromethoxy.[13] Therefore, the independence of the rate of disappearance of $Ru(cp)_2Cl$ on oxygen (Table I) and the reaction of trichloromethyl radicals with oxygen reinforce our proposition (see above) of unrelated paths for the transformations of $\cdot CCl_3$ and $Ru(cp)_2Cl$. Since the fate of the trichloromethyl radical in flash photolysis of deaerated solutions seems to be largely determined by reaction 5, the initial concentration of $Ru(cp)_2Cl$ can be obtained from the concentration of the product, $Ru(cp)_2Cl^+$, and an appropriate mass balance.[15] Such estimation gives an extinction $\epsilon \approx 3.0 \times 10^3$ M^{-1} cm^{-1} for ruthenocenium at $\lambda_{max} = 360$ nm and a rate constant $k = (3.2 \times 0.6) \times 10^9$ M^{-1} s^{-1} for the disproportionation (eq 2).

(13) It must be noticed that the new product(s) can be produced through the addition of oxygenated radicals to the cyclopentadienyl ring as in the case of ferrocene.[14]

(14) Akiyama, T.; Sugimori, A.; Herman, H. *Bull. Chem. Soc. Jpn.* **1973**, *46*, 1855.

(15) The mass balance was based on the final concentration of $Ru(cp)_2Cl^+$. This was evaluated in flash photolysis from the absorbance change at large reaction times and the extinction coefficient of $Ru(cp)_2Cl^+$, $\epsilon = 1.28 \times 10^3$ M^{-1} cm^{-1}, measured at 360 nm.

Experimental Section

Photochemical Procedures. Steady-state irradiations of ruthenocene in various solvents were limited to conversions to products smaller than 1% in order to avoid problems associated with photolysis of the products.[9] Quasi-monochromatic light, half band width ~10 nm at medium height, was obtained by using a setup consisting of a 1-kW high-pressure xenon lamp, a Bausch and Lomb grating monochromator, and focusing optics. The solutions of the ruthenium complex were deaerated with streams of Ar.

The apparatus and procedures used for conventional and laser flash photolysis have been described elsewhere.[16] The raw data were processed in a Digital PDP-11 computer for the study of reaction kinetics and the obtainment of spectral information. Kinetics were investigated by curve fitting after the derivation of the corresponding first- or second-order rate constants by a least-squares treatment of the data points. Moreover, the results of this procedure were routinely verified by investigating the dependence of the reaction half-lifetime on transient concentration.

Electrochemical Procedures. The electrochemical oxidation of ruthenocene was carried out at a Pt electrode with 0.2 M $LiClO_4$ as support electrolyte in acetonitrile. Deaerated solutions of the complex were placed in a three-electrode cell, and the potential of the working electrode was adjusted to values that ensured the oxidation of 99.9% of the complex[4,5] yet were maintained conveniently low in order to avoid further electrochemical reactions. The electrode potential was maintained at the desired value, with respect to a saturated calomel electrode, by means of a potentiostat, and the electrolysis was followed by means of the current. Current vs. time curves, automatically integrated in a calibrated strip-chart recorder with an integrator, gave the charge delivered at the working electrode during the electrolysis. The addition of stoichiometric amounts of $(CH_3)_4N \cdot Cl$, $(C_2H_5)_4N \cdot Br$, or $LiBr_3$ (in acetonitrile) to electrolyzed solutions of ruthenocene produced the spectral changes that were expected for the formation of $Ru(cp)_2X^+$, $X = Cl^-$, Br^-, or Br_3^-.

Materials. Ruthenocene was purchased from Strem Chemicals and purified by sublimation under vacuum. The purity was checked by means of the optical spectrum.

The liquids used as solvents for photochemical and electrochemical experiments, namely CCl_4, cyclohexane, and CH_3CN, were purified by distillation in an all-gas apparatus provided with a 70-theoretical-plate fractionating column. Other materials were reagent grade and used without further purification.

Acknowledgment. The research described herein was supported by the Office of Basic Energy Sciences of the Department of Energy. This is Document No. NDRL-2494 from the Notre Dame Radiation Laboratory.

Registry No. $Ru(cp)_2$, 1287-13-4; $Ru(cp)_2Cl^+$, 51376-92-2; $Ru(cp)_2Br^+$, 54438-59-4; $Ru(cp)_2Cl$, 90388-61-7.

Supplementary Material Available: Figure 1, a comparison of the spectra of $Ru(cp)_2X^+$ produced in electrochemical and photochemical oxidations of ruthenocene (1 page). Ordering information is given on any current masthead page.

(16) Prasad, D. R.; Ferraudi, G. *Inorg. Chem.* **1983**, *22*, 1672.